



1 **Organic amine weakens chloride depletion in coastal**
2 **atmosphere**

3 Aijing Song¹, Kun Li¹, Zhaomin Yang¹, Li Xu², Narcisse Tsoma Tchinda¹, and Lin
4 Du^{1,2,3,*}

5 ¹Qingdao Key Laboratory for Prevention and Control of Atmospheric Pollution in Coastal Cities,
6 Environment Research Institute, Shandong University, Qingdao 266237, China

7 ²School of Environmental Science and Engineering, Shandong University, Qingdao 266237, China

8 ³State Key Laboratory of Microbial Technology, Shandong University, Qingdao 266237, China

9 *Correspondence to: Lin Du (lindu@sdu.edu.cn)*

10 _____



11 **Abstract.** Chloride depletion from sea salt aerosols (SSA) has frequently been observed in polluted
12 coastal regions, severely impacting air quality and human health. However, the influencing mechanism
13 of alkaline species in chloride depletion remains incompletely understood. Here, we report the first
14 investigation of alkaline species including NH₃ and an organic amine (dimethylamine, DMA) on
15 chloride depletion and the subsequent formation of organic chlorinated compounds. Results showed
16 that alkaline species could weaken chloride depletion caused by acidic gases, mainly due to acid-base
17 neutralization. Specifically, chloride depletion in the presence of NO_x decreased from 20.1% to 15.8%
18 when NH₃ concentration increased from 100 to 300 ppb. Chloride depletion also decreased from 18.6%
19 to 13.5% with DMA concentration increasing from 50 to 150 ppb. The weakening effect of organic
20 amine on chloride depletion is more pronounced than that of NH₃, primarily because DMA has stronger
21 alkalinity and nucleation ability. These alkaline species exhibit a stronger reduction of chloride
22 depletion in the presence of SO₂ than in the presence of NO_x. The detection of organic chlorinated
23 products, which were formed via active chlorine-induced oxidation, is consistent with the role of
24 alkaline species in weakening chloride depletion. The formation of organic chlorinated compounds was
25 weakened by the addition of alkaline species, indicating the significant role of alkaline species in
26 reducing active chlorine. These findings suggest that alkaline species, more specifically organic amines,
27 are significant factors influencing chloride depletion in the coastal atmosphere. This further enhances
28 our understanding of chloride depletion phenomena in coastal regions.

29 **1 Introduction**

30 Sea salt aerosols (SSA), primarily composed of sodium chloride, are abundant in coastal areas and play
31 a key role in cloud nucleation with high light scattering efficiency (Zhang and Chan, 2023; Zhou et al.,
32 2025). Chloride depletion, which refers to the removal of chloride ions from SSA, has been frequently
33 observed in the coastal atmosphere (Bian et al., 2014; Duan et al., 2024; Su et al., 2022). Chloride
34 depletion in SSA accelerates their aging process, profoundly influencing visibility, global climate and
35 the earth-atmosphere radiative balance (Ghosh et al., 2020; Edwards et al., 2024; Su et al., 2022). This
36 process also affects the atmospheric oxidation capacity by producing Cl₂, HCl, Cl[•], and other reactive
37 species (Hoffmann et al., 2019; Chen et al., 2024b; Dai et al., 2025). However, significant
38 discrepancies exist between field observations and model predictions of chloride depletion (Nolte et al.,



39 2008; Nolte et al., 2015), highlighting the need for a deeper understanding of its underlying
40 mechanisms.

41 Alkaline species such as NH₃ and organic amines have been suspected to affect chloride depletion (Su
42 et al., 2022). Gaseous ammonia (NH₃), the most abundant alkaline species in the atmosphere, plays an
43 important role in the formation of atmospheric particles (Behera et al., 2013; Lan et al., 2024; Wang et
44 al., 2020). A field study found a relatively low level of chloride depletion in the Antarctic winter, and
45 the large amount of ammonia emitted by penguins has been hypothesized to be responsible for this
46 phenomenon (Rankin and Wolff, 2003). Dimethylamine (DMA, (CH₃)₂NH), a predominant organic
47 amine in the atmosphere, has stronger alkalinity than ammonia and could compete with ammonia in
48 reactions with acidic species, despite its atmospheric concentration being much lower than that of
49 ammonia (Chen et al., 2022; Xie et al., 2018; Liu et al., 2024a). However, to the best of our knowledge,
50 there is currently no experimental evidence illustrating the role of alkaline species in chloride
51 depletion.

52 Organic chlorinated compounds are important indicators of chloride depletion. They can be formed
53 from the oxidation of volatile organic compounds (VOCs) by reactive chlorine species (e.g., Cl[•], Cl₂^{•-},
54 etc.) generated during the chloride depletion process (Zhang and Chan, 2023; Wennberg et al., 2018;
55 Wang et al., 2022b). Once formed, some organic chlorinated compounds with low volatility can
56 partition into the particle phase, contributing to the formation of secondary organic aerosols (SOA). For
57 example, it is estimated that organic chlorinated compounds can contribute up to 15% of total SOA in
58 polluted areas with sufficient chlorine and VOC emissions (Liu et al., 2024b). Organic chlorinated
59 compounds have been observed during chloride depletion in our previous study in the presence of
60 isoprene (Song et al., 2025), a significant biogenic VOC emitted from ocean and terrestrial plants (Yu
61 and Li, 2021; Zhang et al., 2025; Zou et al., 2023). Studying the formation of organic chlorinated
62 compounds not only characterizes the influence of alkaline species on chloride depletion but also holds
63 significant implications for the chlorine cycle.

64 To investigate the roles of alkaline species, including NH₃ and organic amine, in chloride depletion,
65 experiments on reactions involving SSA particles, alkaline species, acidic gases, and/or isoprene were
66 conducted in a chamber. We characterized the changes in chloride depletion and further analyzed the
67 subsequent formation of corresponding organic chlorinated compounds to explore the reasons for their
68 changes. This study provides a comprehensive understanding of chloride depletion from SSA, which



69 may be crucial for more accurately predicting chloride depletion in coastal atmospheres.

70 **2 Materials and methods**

71 **2.1 Chamber experiments**

72 To study the effect of alkaline species on chloride depletion, three groups of experiments were designed:
73 NaCl particles + NH₃/DMA (control experiments), NaCl particles + H₂O₂ + NO_x/SO₂ + NH₃/DMA,
74 and NaCl particles + H₂O₂ + isoprene + NO_x/SO₂ + NH₃/DMA. Details of experimental conditions are
75 provided in Table 1. All experiments were conducted in a 1.5 m³ indoor chamber consisting of 60 µm
76 Teflon film within a temperature-controlled environment, surrounded by black light lamps (F40BLB,
77 GE) with the center irradiation wavelength of 365 nm as the light source. The chamber was equipped
78 with a set of online instruments for measuring physical and chemical parameters. The concentration of
79 aerosol particles was measured using a scanning mobility particle sizer (SMPS, Grimm, Germany),
80 which is composed of a differential mobility analyzer (DMA, 55-L, Grimm, Germany) and a
81 condensation particle counter (CPC, 5416, Grimm, Germany). The concentrations of NO_x and isoprene
82 in the chamber were monitored using a NO-NO₂-NO_x analyzer (Model 42i, Thermo Scientific, USA)
83 and a gas chromatograph coupled with a flame ionization detector (GC-FID 7890B, Agilent
84 Technologies, USA). H₂O₂ acted as the source of OH radicals. The initial concentrations of other
85 substances (H₂O₂, alkaline gases, etc.) were calculated based on the chamber volume and the injection
86 volume.

87 **Table 1. Summary of experimental conditions and results.**

Experiment ^a	[Isoprene] ₀ (ppb)	[H ₂ O ₂] ₀ (ppm)	[NO _x] ₀ (ppb)	[SO ₂] ₀ (ppb)	[NH ₃] ₀ (ppb)	[DMA] ₀ (ppb)	RH (%)	T (°C)	Cl ⁻ /Na ⁺ (mM/mM) ^c
C.1					100		72	20	0.989±0.019
C.2					100		71	20	0.994±0.020
N.1	4	141				69	23		0.755±0.015
NA.1	4	138		100		69	21		0.798±0.016
NA.2	4	139		200		72	21		0.822±0.017
NA.3	4	139		300		72	20		0.841±0.017



ND.1	4	146		50	69	21	0.813±0.017	
ND.2	4	147		100	71	21	0.849±0.017	
ND.3	4	141		150	71	22	0.864±0.018	
S.1	4	300			67	22	0.704±0.009	
SA.1	4	300	100		70	23	0.825±0.017	
SA.2	4	300	200		70	23	0.839±0.017	
SA.3	4	300	300		69	23	0.849±0.017	
SD.1	4	300		50	70	22	0.851±0.017	
SD.2	4	300		100	71	22	0.865±0.018	
SD.3	4	300		150	70	23	0.878±0.018	
IN.1 ^b	667	4	150		72	20	0.770±0.016	
INA.1 ^b	621	4	140	100		71	22	0.784±0.016
INA.2	604	4	161	300		69	23	0.791±0.016
IND.1 ^b	601	4	152		100	68	22	0.814±0.017
IND.2	668	4	146		150	70	20	0.866±0.018
IS.1 ^b	776	4	300		68	20	0.655±0.008	
ISA.1 ^b	604	4	300	100		70	20	0.790±0.016
ISA.2	601	4	300	300		71	21	0.800±0.016
ISD.1 ^b	629	4	300		100	70	21	0.897±0.018
ISD.2	594	4	300		150	69	22	0.961±0.020

88 ^aAbbreviations used in experimental codes correspond to the reactants introduced into the chamber.

89 “N”, “S”, “A”, “D”, and “I” stand for NO_x, SO₂, NH₃, DMA, and isoprene, respectively. C.1 and C.2
90 are control experiments.

91 ^bExperiments were repeated to collect aerosol particles for composition measurement by
92 UPLC/ESI-HR-Q-TOFMS.

93 ^cErrors in Cl⁻/Na⁺ were calculated by error propagation considering Cl⁻ and Na⁺ errors derived from
94 their IC calibration curve.

95 The chamber was thoroughly cleaned using O₃ and purified air, and exposed to UV lamps for at least
96 12 h before each experiment. Relative humidity (RH) in the chamber was adjusted by the proportion of
97 dry and wet air. Subsequently, SSA particles produced by atomizing NaCl solution with an atomizer
98 (Model 3076, TSI, USA) were introduced into the chamber. Based on the experimental design, known



99 volumes of other reactants (i.e., H₂O₂ (Aladdin, 30 wt% in H₂O), inorganic gases (NH₃, NO, etc)
100 (Qingdao Deyi Gas Company, 500 ppm balanced in N₂), DMA (Aladdin, 40 wt% in H₂O), and isoprene
101 (Macklin, >99%)) were introduced into the chamber. After the reactants were adequately mixed for 20
102 minutes, the black light lamps were turned on to initiate the reaction. The experiment lasted for two
103 hours, after which aerosol particles generated during the experiment were collected onto quartz filters
104 and 47 mm polytetrafluoroethylene (PTFE) filters and stored at -20 °C until offline analysis.

105 **2.2 Particle analysis**

106 The concentrations of inorganic ions were measured by ion chromatography (IC, Dionex ICS-600,
107 Thermo Scientific, USA). Aerosol particles collected on the quartz filters were first extracted in 5 mL
108 of ultrapure water (Milli-Q, Millipore, France) by ice sonication for 45 min. The extract was then
109 filtered through a 0.22 µm polyethersulfone syringe filter and injected into the ion chromatography
110 instrument via a six-way valve with a 250-µL loop. The separation of anions and cations was achieved
111 using a Dionex IonPac AS19 column (4 × 250 mm) with an AG19 guard column (4 × 50 mm, Dionex
112 Ionpac) for anions, and a Dionex IonPac CS12A column (4 × 250 mm) with a CG12A guard column (4
113 × 50 mm, Dionex Ionpac) for cations. A 20 mM potassium hydroxide solution was used as the anionic
114 eluent, while a 20 mM methanesulfonic acid solution was employed for cationic elution. The flow rate
115 for both eluents was maintained at 1 mL min⁻¹. The degree of chloride depletion was characterized by
116 the mole ratios of Cl⁻/Na⁺. The Cl⁻/Na⁺ value for fresh SSA is around 0.99, while lower Cl⁻/Na⁺ ratios
117 in SSA indicate the occurrence of chloride depletion.

118 The formation of organic chlorinated compounds was characterized using ultra-high performance
119 liquid chromatography (UPLC, UltiMate 3000, Thermo Scientific, USA) coupled with electrospray
120 ionization high-resolution quadrupole time-of-flight mass spectrometer (ESI-HR-Q-TOF-MS, Bruker
121 Impact HD, Germany). Prior to measurements, aerosol particles collected on PTFE filters were
122 extracted twice using 5 mL methanol (Optima® LC/MS grade, Fisher Scientific, USA) by sonication in
123 an ice bath for 30 min. The extract was filtered through a PTFE syringe filter (0.22 µm) to remove
124 impurities, and then concentrated under a gentle nitrogen gas (99.999%, DEYI). The dried extract was
125 reconstituted in 200 µL of a 1:1 (v:v) mixture of methanol and ultrapure water containing 0.1% formic
126 acid (Optima® LC/MS grade, Fisher Scientific, USA). Sample extracts (10 µL) were analyzed using an
127 Atlantis T3 C18 column (100 Å, 3 µm particle size, 2.1 mm × 150 mm, Waters, USA). The mobile



128 phase comprised 0.1% formic acid in ultrapure water (A) and 0.1% formic acid in methanol (B). A 60
129 min gradient elution with a flow of 200 $\mu\text{L min}^{-1}$ was performed as follows: B initially maintained at 3%
130 for the first 3 minutes, gradually increased to 50% from 3 to 25 minutes, and then rose to 90% from 25
131 to 43 minutes. The fraction of B was reduced back to 3% between 43 and 48 minutes, and maintained
132 at 3% until 60 minutes to re-equilibrate the column.

133 Mass spectrometric data were analyzed with Bruker Compass Data Analysis version 4.2 Build 383.1
134 software. The molecular formulas of organic chlorinated compounds were assigned as
135 $\text{C}_{2-40}\text{H}_{2-80}\text{O}_{0-40}\text{N}_{0-3}\text{S}_{0-2}\text{Cl}_{1-2}$ within a ± 5 ppm mass tolerance, with restrictive conditions applied to
136 exclude unreasonable formulas: $1 \leq \text{H/C} \leq 3$, $0.2 \leq \text{O/C} < 1.5$, $0 \leq \text{N/C} \leq 0.5$, $0 \leq \text{S/C} \leq 1$, $\text{S/O} \leq 0.25$, 0
137 $<$ double bond equivalent (DBE)/C < 1 . The organic chlorinated compounds were reliably identified
138 based on their isotopic mass and intensity, but the identified formulas containing isotopes (e.g., ^{13}C , ^{18}O ,
139 ^{34}S , and ^{37}Cl) were not further discussed. The carbon oxidation state (OS_C) and DBE of the assigned
140 molecular formula ($\text{C}_\text{c}\text{H}_\text{h}\text{O}_\text{o}\text{N}_\text{n}\text{S}_\text{s}\text{Cl}_\text{j}$) were calculated as follows:

$$141 \quad \text{DBE} = 1 + \frac{2\text{C} - (\text{H} + \text{J}) + \text{n}}{2} \quad (1)$$

$$142 \quad \text{OS}_\text{C} \approx 2 \times \frac{\text{O}}{\text{C}} - \frac{\text{H}}{\text{C}} \quad (2)$$

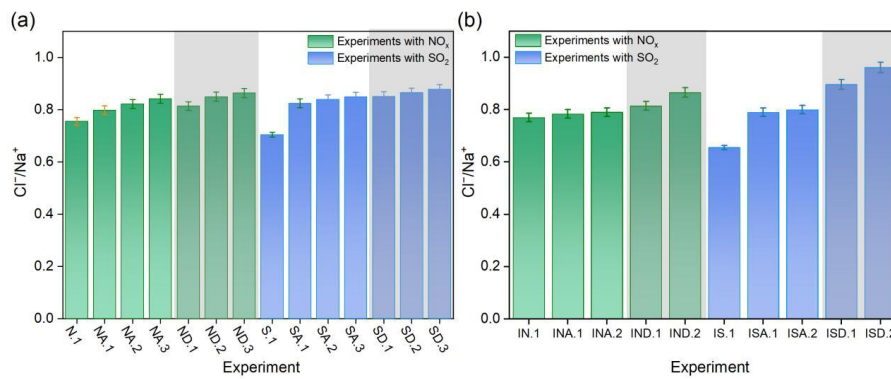
143 **3. Results and discussion**

144 **3.1 Effects of NH_3 on chloride depletion**

145 A series of experiments were designed with varying initial concentrations of alkaline species in the
146 presence of acid gases, i.e., SO_2 and NO_x , to evaluate the effect of alkaline species on chloride
147 depletion (Table 1). Despite NH_3 addition in the absence of SO_2 and NO_x had little effect on chloride
148 depletion (Exp.C.1), it could significantly reduce chloride depletion caused by NO_x and SO_2 (Fig. 1a).
149 For example, the mole ratios of Cl^-/Na^+ increased from 0.798 to 0.841 when the concentration of NH_3
150 raised from 100 to 300 ppb under constant NO_x (Exp.NA.1-NA.3), while this ratio was 0.755 when
151 only NO_x was present (Exp.N.1). This corresponds to a reduction in chloride depletion from 20.1% to
152 15.8%. In these experiments, nitric acid (HNO_3) could be produced either through $\text{NO}_2 + \text{OH}$ reaction
153 or through $\text{N}_2\text{O}_5 + \text{H}_2\text{O}$ reaction, which can cause chloride depletion through the replacement reaction
154 (Su et al., 2022; Xu et al., 2021). The suppressed chloride depletion by NH_3 can be attributed to the
155 neutralization reaction between NH_3 and HNO_3 that generates NH_4NO_3 particles (Behera et al., 2013).



156 Although NH_4NO_3 is unstable (Behera et al., 2013; Lan et al., 2024), ammonium ions were detected in
157 these experiments. In the presence of SO_2 , the effect of NH_3 on reducing chloride depletion is even
158 more pronounced. For example, the addition of 300 ppb NH_3 (Exp.SA.3) reduced SO_2 -induced chloride
159 depletion from 29.5% (Exp.S.1) to 15.0%. This can be explained by the generation of $(\text{NH}_4)_2\text{SO}_4$ via
160 the reaction of NH_3 with sulfuric acid (H_2SO_4), which is produced from the oxidation of SO_2 by OH
161 radicals (Lan et al., 2024; Behera et al., 2013). As shown in Fig. S1, ammonium ion was detected in
162 Exp.SA.1-SA.3. Notably, the affinity for the reaction between H_2SO_4 and NH_3 is much greater than that
163 between HNO_3 and NH_3 (Behera et al., 2013), and the reaction rate between H_2SO_4 and NH_3 is higher
164 than that between HNO_3 and NH_3 (Behera and Sharma, 2011). This may be the reason why the
165 reduction in chloride depletion was more significant in experiments SA.1-SA.3 compared to
166 experiments NA.1-NA.3.



167

168 **Figure 1. Dependences of Cl^-/Na^+ ratio on the concentrations of various alkaline species in the (a) absence**

169 and (b) presence of isoprene. The experiments with a grey background represent the addition of DMA.

170 Isoprene was further introduced into the experimental chamber with various initial NH_3 concentrations
171 to study the combined effect of alkaline gases with isoprene and acidic gases (Fig. 1b). Similar to the
172 above experiments without isoprene, NH_3 can reduce the chloride depletion caused by acidic gases,
173 with a more pronounced weakening effect in the presence of SO_2 . Notably, the addition of isoprene
174 reduced the ability of NH_3 to weaken chloride depletion, resulting in relatively enhanced chloride
175 depletion. For instance, chloride depletion was 20.8% in the experiment with isoprene and NH_3
176 (Exp.INA.2), significantly higher than 15.8% in the experiment without isoprene (Exp.NA.3). Chloride
177 depletion in Exp.ISA.2 and Exp.SA.3 was 19.9% and 15.0%, respectively, which can be attributed to
178 the reaction of NH_3 with SOA constituents such as organic acids, or other species generated from the



179 oxidation of isoprene to form nitrogen-containing organic compounds (Li et al., 2024; Wu et al., 2021;
180 Wennberg et al., 2018; Bates et al., 2023). This leads to reduced NH₃ for neutralizing acid-induced
181 chloride depletion.

182 **3.2 Effects of DMA on chloride depletion**

183 To further investigate the influence of organic amine, DMA was introduced into the reaction system.
184 Similar to NH₃, DMA also caused negligible chloride depletion in the absence of acidic gases (Exp.C2,
185 Table 1). In the presence of acidic gases, the weakening effect of chloride depletion becomes more
186 pronounced with increasing DMA concentrations (Fig. 1a). For example, chloride depletion decreased
187 from 18.6% to 13.5% as DMA concentration increased from 50 to 150 ppb in the presence of NO_x
188 (Exp.ND.1-ND.3). Chloride depletion in the presence of SO₂ in Exp.SD.1-SD.3, ranging from 12.1%
189 to 14.8%, was higher than that in Exp.S.1 (29.5%). This is mainly because DMA, with a high vapor
190 pressure, can react with inorganic acids (e.g., HNO₃, H₂SO₄, etc.) produced during the reaction to form
191 amine salts with lower vapor pressure (Wang et al., 2010; Murphy et al., 2007; Nielsen et al., 2012).
192 Moreover, DMA can effectively promote cluster formation with H₂SO₄ or HNO₃, thereby generating
193 DMA-H₂SO₄, DMA-H₂SO₄-H₂O, and other nucleation systems (Chen et al., 2024a; Loukonen et al.,
194 2010; Zhang et al., 2019). The aforementioned mechanisms can all reduce chloride depletion caused by
195 inorganic acids.

196 As shown in Fig. 1a, chloride depletion in Exp.ND.2 (15.0%) was lower than that in Exp.NA.1 (20.1%).
197 In Exp.SD.2, chloride depletion was 13.4%, which was also lower than 17.4% in Exp.SA.1. Despite the
198 concentration of DMA is lower than that of NH₃, chloride depletion in the presence of DMA (Exp.SD.1)
199 was still lower than that in the presence of NH₃ (Exp.SA.1). It follows that the weakening effect of
200 DMA on chloride depletion is significantly greater than that of NH₃, and this can be attributed to the
201 stronger alkalinity of DMA compared to NH₃ (Chen et al., 2022; Sauerwein and Chan, 2017; Xie et al.,
202 2018). Furthermore, the clusters formed by DMA and HSO₄ are more stable than those formed by NH₃
203 and H₂SO₄ (Ortega et al., 2012; Kupiainen et al., 2012). According to a theoretical study by Zhang et al.
204 (2019), DMA is more likely to approach the air-nanoparticle interface compared to NH₃, where the
205 probability of its heterogeneous reaction with H₂SO₄ can increase.

206 Following the addition of isoprene, the weakening effect of DMA on chloride depletion in the presence
207 of NO_x was not significantly different from that of experiments without isoprene. Nonetheless, this



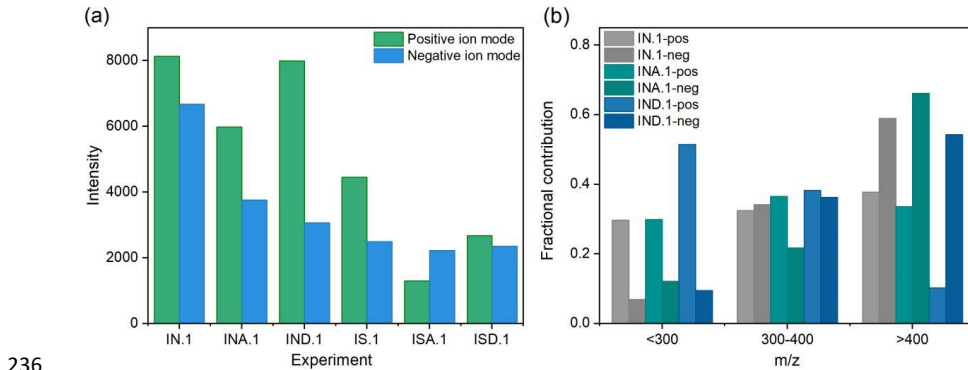
208 addition enhanced the weakening effect of DMA on chloride depletion in the presence of SO_2 . Chloride
209 depletion in Exp.ISD.2 was 3.8%, significantly lower than that in Exp.SD.3 (12.1%). This can be
210 explained by the fact that organic acids produced from the oxidation of isoprene enhance DMA- H_2SO_4
211 nucleation, with a stronger enhancement effect observed at lower H_2SO_4 concentrations (Wang et al.,
212 2022a; Lu et al., 2020). Isoprene oxidation products can react with H_2SO_4 to form organic sulfates
213 (Armstrong et al., 2022; Wach et al., 2020), leading to a reduction in H_2SO_4 concentration within the
214 reaction system.

215 **3.3 Formation of organic chlorinated compounds**

216 The molecular composition of organic chlorinated compounds was analyzed, using
217 UPLC/ESI-Q-TOF-MS, to further explore the effect of active chlorine on chloride depletion. Fig. S2
218 presents the mass spectra of organic chlorinated compounds in the presence of acidic and alkaline gases.
219 Mass spectra in both positive and negative ion modes contained numerous peaks, with more complex
220 compositions in the presence of NO_x compared to those in the presence of SO_2 .

221 **3.3.1 Effects of alkaline species in the presence of NO_x**

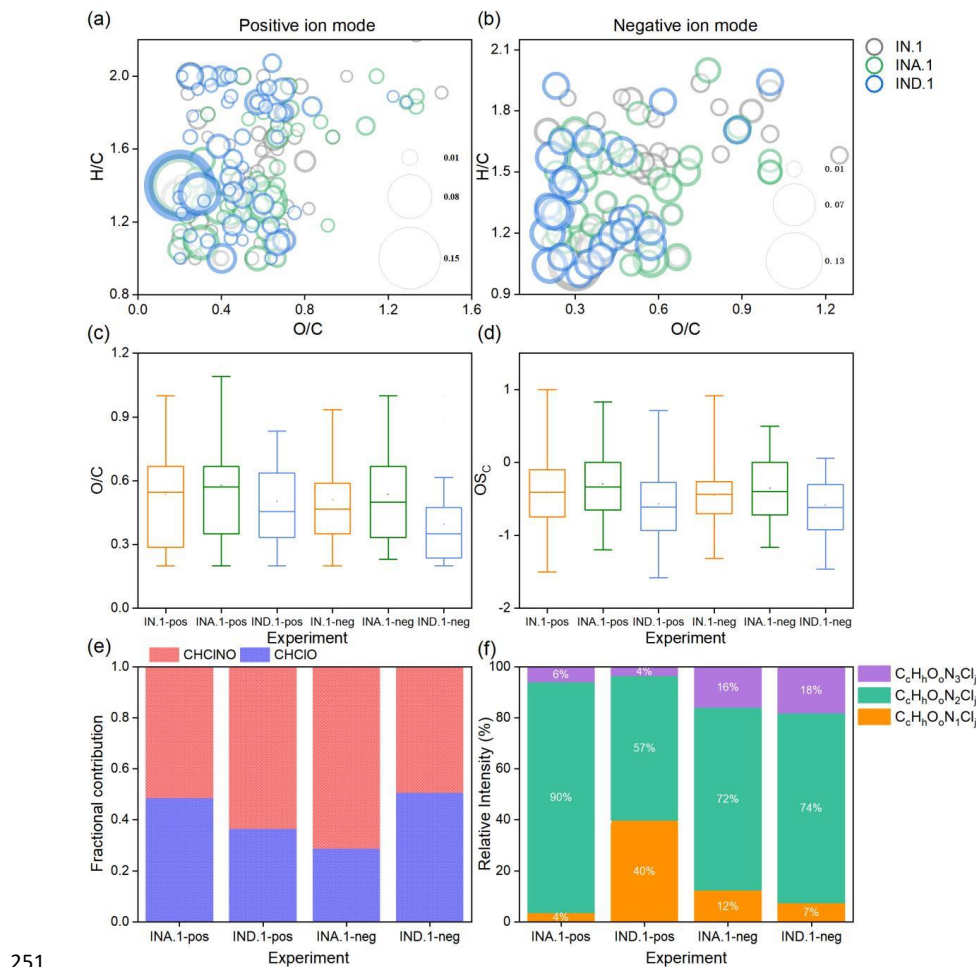
222 As shown in Fig. 2a, the total signal intensity of the organic chlorinated compounds detected in the
223 presence of alkaline species (Exp.INA.1 and Exp.IND.1) was lower than that in their absence
224 (Exp.IN.1), indicating that the alkaline species reduce the formation of organic chlorinated compounds
225 during the chloride depletion process. The identified organic chlorinated compounds were classified
226 into three categories: $\text{m/z} < 300$, $300 \leq \text{m/z} \leq 400$ and $\text{m/z} > 400$ (Fig. 2b). The molecular weight
227 distribution of products shifted with the addition of alkaline species. In the experiment without alkaline
228 species (Exp.IN.1), molecules with high molecular weight ($\text{m/z} > 400$) had the highest proportion. In
229 contrast, DMA reduced the proportion of high molecular weight molecules ($\text{m/z} > 400$), while
230 increasing the intensity of molecules with m/z values in the ranges $\text{m/z} < 300$ and $300 \leq \text{m/z} \leq 399$
231 (Exp.IND.1) as shown in Fig. 2b. This suggests that the presence of DMA facilitates the formation of
232 organic chlorinated compounds with lower molecular weight, which can be attributed to the stronger
233 neutralization of the acidity by DMA, thereby inhibiting the acid-catalyzed polymerization reaction to
234 generate high molecular weight molecules (Du et al., 2023). The lower proportion of organic
235 chlorinated oligomers produced in Exp.IND.1 further supports this speculation (Fig.S3).



236

237 **Figure 2. (a) Total signal intensity of identified organic chlorinated compounds for different experiments. (b)**
238 **Distribution of identified molecules under different experimental conditions.**

239 The Van Krevelen (VK) diagrams based on O/C and H/C ratios are presented in Fig. 3a-3b. The H/C
240 and O/C ratios of organic chlorinated compounds are primarily distributed in the ranges of 0.9-2.0 and
241 0.1-1.0. As shown in Fig. 3c, the organic chlorinated compounds produced in the presence of NH₃
242 (Exp.INA.1) exhibited the highest O/C ratio, which can be attributed to the presence of more hydroxyl,
243 carbonyl, and carboxyl functional groups. The OSC of organic chlorinated compounds in Exp.INA.1
244 was also higher, indicating that NH₃ enhances the degree of oxidation of organic chlorinated
245 compounds (Fig. 3d). Conversely, the O/C ratio and OSC of organic chlorinated compounds were low
246 in the presence of DMA (Exp.IDA.1). Fig. S4 shows that the proportion of dichlorinated compounds in
247 the presence of DMA is lower than that in the presence of NH₃, indicating that less active chlorine was
248 produced in the presence of DMA and its multi-generation oxidation was inhibited. This result further
249 supports that the weakening effect of DMA on chloride depletion is significantly higher than that of
250 NH₃ as mentioned above.

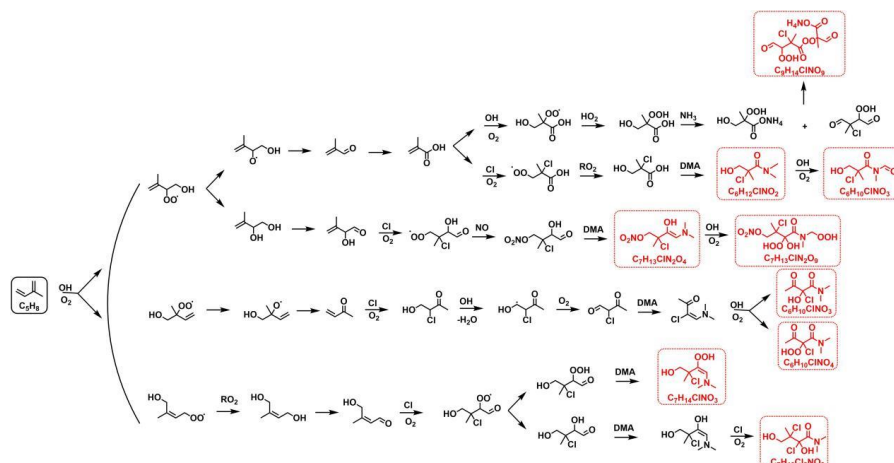


251
 252 **Figure 3. Van Krevelen diagram of organic chlorinated compounds for different experiments with NO_x in the**
 253 **(a) positive and (b) negative ion modes. The circle size represents the proportion of organic chlorinated**
 254 **compounds. (c) OSC and (d) DBE of organic chlorinated compounds for different experiments with NO_x . (e)**
 255 **Fractional contribution to the total unique molecules by CHClO and CHClNO compounds in the presence of**
 256 **alkaline species. (f) Nitrogen atom distribution of CHClNO compounds in the presence of alkaline species for**
 257 **different experiments with NO_x .**

258 Furthermore, we compared the chemical composition of organic chlorinated compounds with and
 259 without alkaline species. As shown in Fig. S5, many unique molecules were detected in the
 260 experiments with alkaline species (Exp.INA.1 and Exp.IND.1), in addition to some compounds also
 261 detected in Exp.IN.1. In the experiment with NH_3 (Exp.INA.1), 42 and 30 unique molecules were
 262 detected in the positive and negative ion modes, respectively. When DMA was present (Exp.IDA.1), 45
 263 and 25 unique organic chlorinated compounds were identified in the positive and negative modes,



264 respectively. These findings suggest that alkaline species alter the molecular composition
265 characteristics of organic chlorinated compounds. These specific molecules predominantly consist of
266 CHClO and CHClNO compounds, with the proportion of CHClNO being higher than that of CHClO
267 (Fig. 3e). The CHClNO compounds primarily consist of N2 products (Fig. 3f), and their formation is
268 favored by high humidity (Yang et al., 2025). Representative CHClNO compounds include
269 $C_9H_{14}ClNO_9$, $C_7H_{13}ClN_2O_4$, $C_6H_{12}ClNO_2$, and others. Fig. 4 presents the formation mechanism of these
270 compounds. Specifically, isoprene is oxidized by OH radicals to form key intermediates, which can be
271 further oxidized by Cl radicals, yielding organic chlorinated monomers (e.g., $C_4H_7ClO_3$, $C_4H_5ClO_2$,
272 $C_5H_9ClO_4$). These monomers can be converted into organic chlorinated oligomers through dehydration
273 reactions or acid-catalyzed accretion reactions. Notably, NH_3 and DMA can react with these organic
274 chlorinated compounds through acid-base neutralization to produce CHClNO compounds. For instance,
275 NH_3 and DMA can react with $C_4H_8O_5$ and $C_4H_7ClO_3$, respectively, to form $C_4H_{11}NO_5$ and $C_6H_{12}ClNO_2$.
276 $C_4H_{11}NO_5$ and $C_5H_9ClO_4$ can undergo an accretion reaction to form $C_9H_{14}ClNO_9$. In addition, DMA
277 can react with the aldehyde function of organic chlorinated compounds to form carbinolamines, which
278 then dehydrate to form enamine compounds (e.g., $C_7H_{13}ClN_2O_4$ and $C_7H_{14}ClNO_2$). These enamine
279 compounds can be further oxidized by OH and Cl radicals to produce the observed CHClNO
280 compounds (e.g., $C_6H_{10}ClNO_3$, $C_7H_{13}Cl_2NO_3$, $C_7H_{13}ClN_2O_9$).

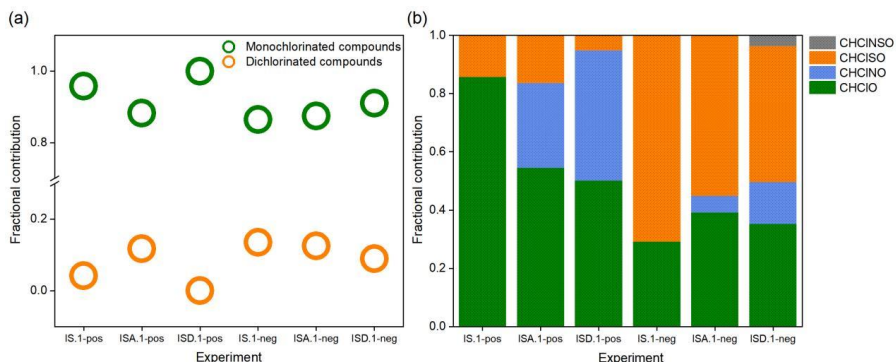


281
282 **Figure 4. (a) Formation mechanism of representative CHClNO compounds. The red boxes indicate the**
283 **detected CHClNO compounds in our experiments.**



284 **3.3.2 Effects of alkaline species in the presence of SO₂**

285 In the presence of SO₂, the addition of NH₃ and DMA both significantly reduced the abundance of high
286 molecular weight compounds (Fig. S6). They also reduced the total signal intensity of organic
287 chlorinated compounds (Fig. 5a), which can be attributed to a reduced activation of chloride ions. This
288 might be due to the fact that the addition of alkaline species reduces the production of gaseous HCl as a
289 result of acid-base neutralization reactions and further diminishes the source of active chlorine
290 (Edwards et al., 2024; Song et al., 2025). In addition, chloride ions can be activated into active chlorine
291 by strong oxidants (OH radicals, O₃, etc.) (Zhang and Chan, 2023; Su et al., 2022). DMA can compete
292 with chloride ions for these oxidants, thereby limiting the activation of chloride ions and reducing the
293 generation of active chlorine species (Møller et al., 2020). The proportion of dichlorinated compounds
294 in Exp.ISD.1 was significantly lower than that in Exp.IS.1 (Fig. 5a), mainly due to the reduction of
295 active chlorine inhibiting its multi-generation oxidation. This further explains that the weakening effect
296 of DMA on chloride depletion is enhanced in the presence of isoprene and SO₂.



297
298 **Figure 5. (a) Fractional contribution of monochlorinated and dichlorinated compounds in the total organic**
299 **chlorinated compounds for different experiments with SO₂. (b) Fractional contribution to the total organic**
300 **chlorinated compounds by different compounds.**

301 As shown in Fig. 5b, in experiments with SO₂, the products detected in the positive ion mode mainly
302 consisted of CHCIO compounds, while the proportion of CHCISO compounds was the highest in the
303 negative ion mode. This may be related to the different sensitivities of the compounds in different ion
304 modes. CHCINO and CHCINSO compounds (including C₇H₁₅ClN₂O₆, C₁₃H₁₉ClN₂O₆, C₁₈H₃₅ClN₂SO₈,
305 etc) were also detected in experiments in the presence of alkaline species and SO₂. As mentioned above,
306 the CHCINO compounds can be formed through the acid-base neutralization reaction or the reaction of
307 DMA with aldehyde function. These compounds can react with H₂SO₄ through esterification reactions



308 to form CHClNSO compounds. The observed higher proportion of CHClNO compounds in Exp.ISD.1
309 than that in Exp.ISA.1 (Fig. 5b) may result from the stronger ability of DMA to react with organic
310 acids or carbonyl compounds (Smith et al., 2021). Moreover, autoxidation via unimolecular reaction,
311 being an important oxidation pathway for DMA in the atmosphere, facilitates the formation of
312 hydroperoxy amides (Møller et al., 2020). Overall, alkaline gases affect the formation of active chlorine
313 during chloride depletion, and alters the composition of organic chlorinated compounds.

314 **4. Conclusions**

315 The complexity of atmospheric pollutants in coastal environments hinders the understanding of the
316 mechanisms influencing chloride depletion. In this study, we explored the detailed effects of NH₃ and
317 DMA on chloride depletion. The results demonstrated that NH₃ and DMA could weaken the chloride
318 depletion induced by acidic gases, with DMA exhibiting a more substantial weakening effect than NH₃.
319 This difference in their impact is primarily due to DMA's stronger alkalinity and nucleation ability,
320 which enable it to interact more effectively with acidic species than NH₃. Although the concentration of
321 organic amines in the atmosphere is lower than that of NH₃, their impact on the chloride depletion
322 phenomenon is essential. The results of the current study reveal that considering only the effects of
323 acidic gases may lead to deviations in the prediction of chloride depletion. Our findings underscore the
324 necessity to discuss the inclusion of alkaline species in the chloride depletion process, especially
325 organic amines.

326 The mass spectrometry results showed that the presence of alkaline species also reduces the formation
327 of organic chlorinated compounds, indicating that the generation of active chlorine is inhibited during
328 chloride depletion. This can be attributed to the fact that the alkaline species reduce the generation of
329 gaseous HCl through acid-base neutralization reactions, and can compete with chloride ions for
330 oxidants, thereby further reducing the production of active chlorine. This further supports the idea that
331 alkaline species could weaken the chloride depletion process. Additionally, the presence of alkaline
332 species, especially DMA, promotes the formation of low-molecular-weight organic chlorinated
333 compounds by neutralizing acidity, thereby inhibiting acid-catalyzed polymerization and the formation
334 of high-molecular-weight compounds. The addition of alkaline species was observed to alter the
335 composition of organic chlorinated compounds, with several identified unique products that were not



336 present under acidic conditions. This suggests that alkaline species not only inhibit chloride depletion
337 but also influence the overall chemical composition of the atmosphere by altering the chlorination
338 pathways of organic compounds. The current results strengthen our understanding of the mechanism
339 influencing chloride depletion, and provide a ground for the future identification of ambient samples.

340 **Data availability**

341 Experimental data are available upon request to the corresponding author.

342 **Supplement**

343 The supplement related to this article is available online at:

344 **Author contributions**

345 LD and AS designed the experiments, and AS carried them out. AS performed data analysis with
346 assistance from LD, KL, and LX. AS wrote the paper with contributions from all co-authors, and
347 co-authors commented on the paper.

348 **Competing interest**

349 The contact author has declared that none of the authors has any competing interests.

350 **Acknowledgements**

351 We thank Guannan Lin from the State Key Laboratory of Microbial Technology of Shandong
352 University for help and guidance with UPLC/ESI-HR-Q-TOF-MS measurements.

353 **Financial support**

354 This work was supported by National Key Research and Development Program of China
355 (2023YFC3706203), National Natural Science Foundation of China (U25A20787, 22376121), and
356 Intramural Joint Program Fund of State Key Laboratory of Microbial Technology
357 (SKLMTIJP-2025-02).



358 **References**

359 Armstrong, N. C., Chen, Y., Cui, T., Zhang, Y., Christensen, C., Zhang, Z., Turpin, B. J., Chan, M. N.,
360 Gold, A., Ault, A. P., and Surratt, J. D.: Isoprene epoxydiol-derived sulfated and nonsulfated oligomers
361 suppress particulate mass loss during oxidative aging of secondary organic aerosol, *Environ. Sci.*
362 *Technol.*, 56, 16611-16620, <https://doi.org/10.1021/acs.est.2c03200>, 2022.

363 Bates, K. H., Jacob, D. J., Cope, J. D., Chen, X., Millet, D. B., and Nguyen, T. B.: Emerging
364 investigator series: Aqueous oxidation of isoprene-derived organic aerosol species as a source of
365 atmospheric formic and acetic acids, *Environ. Sci.: Atmos.*, 3, 1651-1664,
366 <https://doi.org/10.1039/d3ea00076a>, 2023.

367 Behera, S. N. and Sharma, M.: Degradation of SO₂, NO₂ and NH₃ leading to formation of secondary
368 inorganic aerosols: An environmental chamber study, *Atmos. Environ.*, 45, 4015-4024,
369 <https://doi.org/10.1016/j.atmosenv.2011.04.056>, 2011.

370 Behera, S. N., Sharma, M., Aneja, V. P., and Balasubramanian, R.: Ammonia in the atmosphere: A
371 review on emission sources, atmospheric chemistry and deposition on terrestrial bodies, *Environ. Sci.*
372 *Pollut. Res.*, 20, 8092-8131, <https://doi.org/10.1007/s11356-013-2051-9>, 2013.

373 Bian, Q., Huang, X. H. H., and Yu, J. Z.: One-year observations of size distribution characteristics of
374 major aerosol constituents at a coastal receptor site in Hong Kong – Part 1: Inorganic ions and oxalate,
375 *Atmos. Chem. Phys.*, 14, 9013-9027, <https://doi.org/10.5194/acp-14-9013-2014>, 2014.

376 Chen, D.-P., Ma, W., Yang, C.-H., Li, M., Zhou, Z.-Z., Zhang, Y., Wang, X.-C., and Quan, Z.-J.:
377 Formation of atmospheric molecular clusters containing nitric acid with ammonia, methylamine, and
378 dimethylamine, *Environ. Sci.: Processes Impacts*, 26, 2036-2050, <https://doi.org/10.1039/d4em00330f>,
379 2024a.

380 Chen, D., Yao, X., Chan, C. K., Tian, X., Chu, Y., Clegg, S. L., Shen, Y., Gao, Y., and Gao, H.:
381 Competitive uptake of dimethylamine and trimethylamine against ammonia on acidic particles in
382 marine atmospheres, *Environ. Sci. Technol.*, 56, 5430-5439, <https://doi.org/10.1021/acs.est.1c08713>,
383 2022.

384 Chen, G., Xu, L., Yu, S., Xue, L., Lin, Z., Yang, C., Ji, X., Fan, X., Tham, Y. J., Wang, H., Hong, Y., Li,
385 M., Seinfeld, J. H., and Chen, J.: Increasing contribution of chlorine chemistry to wintertime ozone
386 formation promoted by enhanced nitrogen chemistry, *Environ. Sci. Technol.*, 58, 22714-22721,



387 <https://doi.org/10.1021/acs.est.4c09523>, 2024b.

388 Dai, J., Wang, T., Shen, H., Xia, M., Sun, W., and Brasseur, G. P.: Significant impact of a daytime
389 halogen oxidant on coastal air quality, *Environ. Sci. Technol.*, 59, 2169-2180,
390 <https://doi.org/10.1021/acs.est.4c08360>, 2025.

391 Du, L., Xu, L., Li, K., George, C., and Ge, M.: NH₃ weakens the enhancing effect of SO₂ on biogenic
392 secondary organic aerosol formation, *Environ. Sci. Technol. Lett.*, 10, 145-151,
393 <https://doi.org/10.1021/acs.estlett.2c00959>, 2023.

394 Duan, Y., Liu, Y., Zhang, K., Li, L., Huo, J., Chen, J., Fu, Q., Gao, Z., Xiu, G., and Hu, T.: Variations of
395 chloride depletion and its impacts on ozone formation: Case study of a coastal area in Shanghai, *Sci.
396 Total Environ.*, 957, 176899, <https://doi.org/10.1016/j.scitotenv.2024.176899>, 2024.

397 Edwards, E.-L., Choi, Y., Crosbie, E. C., DiGangi, J. P., Diskin, G. S., Robinson, C. E., Shook, M. A.,
398 Winstead, E. L., Ziembka, L. D., and Sorooshian, A.: Sea salt reactivity over the northwest Atlantic: An
399 in-depth look using the airborne ACTIVATE dataset, *Atmos. Chem. Phys.*, 24, 3349-3378,
400 <https://doi.org/10.5194/acp-24-3349-2024>, 2024.

401 Ghosh, A., Roy, A., Das, S. K., Ghosh, S. K., Raha, S., and Chatterjee, A.: Identification of most
402 preferable reaction pathways for chloride depletion from size segregated sea-salt aerosols: A study over
403 high altitude Himalaya, tropical urban metropolis and tropical coastal mangrove forest in eastern India,
404 *Chemosphere*, 245, 125673, <https://doi.org/10.1016/j.chemosphere.2019.125673>, 2020.

405 Hoffmann, E. H., Tilgner, A., Wolke, R., and Herrmann, H.: Enhanced chlorine and bromine atom
406 activation by hydrolysis of halogen nitrates from marine aerosols at polluted coastal areas, *Environ. Sci.
407 Technol.*, 53, 771-778, <https://doi.org/10.1021/acs.est.8b05165>, 2019.

408 Kupiainen, O., Ortega, I. K., Kurtén, T., and Vehkämäki, H.: Amine substitution into sulfuric acid –
409 ammonia clusters, *Atmos. Chem. Phys.*, 12, 3591-3599, <https://doi.org/10.5194/acp-12-3591-2012>,
410 2012.

411 Lan, Z., Lin, W., and Zhao, G.: Sources, variations, and effects on air quality of atmospheric ammonia,
412 *Curr Pollution Rep.*, 10, 40-53, <https://doi.org/10.1007/s40726-023-00291-6>, 2024.

413 Li, X., Jia, L., Xu, Y., and Pan, Y.: A novel reaction between ammonia and Criegee intermediates can
414 form amines and suppress oligomers from isoprene, *Sci. Total Environ.*, 956, 177389,
415 <https://doi.org/10.1016/j.scitotenv.2024.177389>, 2024.

416 Liu, M., Wang, X., Liu, Z., Jiang, Y., Li, M., Zhang, J., Sun, Y., Zhu, Y., Xue, L., and Wang, W.:



417 Characteristics and origins of fine particulate amines at a coastal mountain site in northern China in
418 spring, *Atmos. Environ.*, 321, <https://doi.org/10.1016/j.atmosenv.2024.120365>, 2024a.

419 Liu, X., Liu, L., Zhang, B., Liu, P., Huang, R.-J., Hildebrandt Ruiz, L., Miao, R., Chen, Q., and Wang,
420 X.: Modeling the global impact of chlorine chemistry on secondary organic aerosols, *Environ. Sci.
Technol.*, 58, 23064-23074, <https://doi.org/10.1021/acs.est.4c05037>, 2024b.

422 Loukonen, V., Kurtén, T., Ortega, I. K., Vehkamäki, H., Pádua, A. A. H., Sellegrí, K., and Kulmala, M.:
423 Enhancing effect of dimethylamine in sulfuric acid nucleation in the presence of water – a
424 computational study, *Atmos. Chem. Phys.*, 10, 4961-4974, <https://doi.org/10.5194/acp-10-4961-2010>,
425 2010.

426 Lu, Y., Liu, L., Ning, A., Yang, G., Liu, Y., Kurtén, T., Vehkamäki, H., Zhang, X., and Wang, L.:
427 Atmospheric sulfuric acid-dimethylamine nucleation enhanced by trifluoroacetic acid, *Geophys. Res.
Lett.*, 47, e2019GL085627, <https://doi.org/10.1029/2019gl085627>, 2020.

429 Møller, K. H., Berndt, T., and Kjaergaard, H. G.: Atmospheric autoxidation of amines, *Environ. Sci.
Technol.*, 54, 11087-11099, <https://doi.org/10.1021/acs.est.0c03937>, 2020.

431 Murphy, S. M., Sorooshian, A., Kroll, J. H., Ng, N. L., Chhabra, P., Tong, C., Surratt, J. D., Knipping,
432 E., Flagan, R. C., and Seinfeld, J. H.: Secondary aerosol formation from atmospheric reactions of
433 aliphatic amines, *Atmos. Chem. Phys.*, 7, 2313–2337, <https://doi.org/10.5194/acp-7-2313-2007>, 2007.

434 Nielsen, C. J., Herrmann, H., and Weller, C.: Atmospheric chemistry and environmental impact of the
435 use of amines in carbon capture and storage (CCS), *Chem. Soc. Rev.*, 41, 6684–6704,
436 <https://doi.org/10.1039/c2cs35059a>, 2012.

437 Nolte, C., Bhave, P., Arnold, J., Dennis, R., Zhang, K., and Wexler, A.: Modeling urban and regional
438 aerosols—Application of the CMAQ-UCD aerosol model to Tampa, a coastal urban site, *Atmos.
Environ.*, 42, 3179-3191, <https://doi.org/10.1016/j.atmosenv.2007.12.059>, 2008.

440 Nolte, C. G., Appel, K. W., Kelly, J. T., Bhave, P. V., Fahey, K. M., Collett Jr., J. L., Zhang, L., and
441 Young, J. O.: Evaluation of the Community Multiscale Air Quality (CMAQ) model v5.0 against
442 size-resolved measurements of inorganic particle composition across sites in North America, *Geosci.
Model Dev.*, 8, 2877-2892, <https://doi.org/10.5194/gmd-8-2877-2015>, 2015.

444 Ortega, I. K., Kupiainen, O., Kurtén, T., Olenius, T., Wilkman, O., McGrath, M. J., Loukonen, V., and
445 Vehkamäki, H.: From quantum chemical formation free energies to evaporation rates, *Atmos. Chem.
Phys.*, 12, 225-235, <https://doi.org/10.5194/acp-12-225-2012>, 2012.



447 Rankin, A. M. and Wolff, E. W.: A year-long record of size-segregated aerosol composition at Halley,
448 Antarctica, *J. Geophys. Res. Atmos.*, 108, 4775, <https://doi.org/10.1029/2003jd003993>, 2003.

449 Sauerwein, M. and Chan, C. K.: Heterogeneous uptake of ammonia and dimethylamine into sulfuric
450 and oxalic acid particles, *Atmos. Chem. Phys.*, 17, 6323-6339,
451 <https://doi.org/10.5194/acp-17-6323-2017>, 2017.

452 Smith, N. R., Montoya-Aguilera, J., Dabdub, D., and Nizkorodov, S. A.: Effect of humidity on the
453 reactive uptake of ammonia and dimethylamine by nitrogen-containing secondary organic aerosol,
454 *Atmosphere*, 12, <https://doi.org/10.3390/atmos12111502>, 2021.

455 Song, A., Li, K., Yang, Z., Tsона Tchinda, N., and Du, L.: Marine volatile organic compounds promote
456 the chloride depletion in sea salt aerosols, *J. Geophys. Res. Atmos.*, 130, e2025JD043495,
457 <https://doi.org/10.1029/2025JD043495>, 2025.

458 Su, B., Wang, T., Zhang, G., Liang, Y., Lv, C., Hu, Y., Li, L., Zhou, Z., Wang, X., and Bi, X.: A review
459 of atmospheric aging of sea spray aerosols: Potential factors affecting chloride depletion, *Atmos.*
460 *Environ.*, 290, 119365, <https://doi.org/10.1016/j.atmosenv.2022.119365>, 2022.

461 Wach, P., Spólnik, G., Surratt, J. D., Blažiak, K., Rudzinski, K. J., Lin, Y.-H., Maenhaut, W.,
462 Danikiewicz, W., Claeys, M., and Szmigielski, R.: Structural characterization of lactone-containing
463 MW 212 organosulfates originating from isoprene oxidation in ambient fine aerosol, *Environ. Sci.*
464 *Technol.*, 54, 1415-1424, <https://doi.org/10.1021/acs.est.9b06190>, 2020.

465 Wang, C., Liu, Y., Huang, T., Feng, Y., Wang, Z., Lu, R., and Jiang, S.: Sulfuric acid–dimethylamine
466 particle formation enhanced by functional organic acids: An integrated experimental and theoretical
467 study, *Phys. Chem. Chem. Phys.*, 24, 23540-23550, <https://doi.org/10.1039/d2cp01671k>, 2022a.

468 Wang, D. S., Masoud, C. G., Modi, M., and Hildebrandt Ruiz, L.: Isoprene–chlorine oxidation in the
469 presence of NO_x and implications for urban atmospheric chemistry, *Environ. Sci. Technol.*, 56,
470 9251-9264, <https://doi.org/10.1021/acs.est.1c07048>, 2022b.

471 Wang, L., Lal, V., Khalizov, A. F., and Zhang, R.: Heterogeneous chemistry of alkylamines with
472 sulfuric acid implications for atmospheric formation of alkylaminium sulfates, *Environ. Sci. Technol.*,
473 44, 2461–2465, <https://doi.org/10.1021/es9036868>, 2010.

474 Wang, M., Kong, W., Marten, R., He, X.-C., Chen, D., Pfeifer, J., Heitto, A., Kontkanen, J., Dada, L.,
475 Kürten, A., Yli-Juuti, T., Manninen, H. E., Amanatidis, S., Amorim, A., Baalbaki, R., Baccarini, A.,
476 Bell, D. M., Bertozi, B., Bräkling, S., Brilke, S., Murillo, L. C., Chiu, R., Chu, B., De Menezes, L.-P.,



477 Duplissy, J., Finkenzeller, H., Carracedo, L. G., Granzin, M., Guida, R., Hansel, A., Hofbauer, V.,
478 Krechmer, J., Lehtipalo, K., Lamkaddam, H., Lampimäki, M., Lee, C. P., Makhmutov, V., Marie, G.,
479 Mathot, S., Mauldin, R. L., Mentler, B., Müller, T., Onnela, A., Partoll, E., Petäjä, T., Philippov, M.,
480 Pospisilova, V., Ranjithkumar, A., Rissanen, M., Rörup, B., Scholz, W., Shen, J., Simon, M., Sipilä, M.,
481 Steiner, G., Stolzenburg, D., Tham, Y. J., Tomé, A., Wagner, A. C., Wang, D. S., Wang, Y., Weber, S. K.,
482 Winkler, P. M., Wlasits, P. J., Wu, Y., Xiao, M., Ye, Q., Zauner-Wieczorek, M., Zhou, X., Volkamer, R.,
483 Riipinen, I., Dommen, J., Curtius, J., Baltensperger, U., Kulmala, M., Worsnop, D. R., Kirkby, J.,
484 Seinfeld, J. H., El-Haddad, I., Flagan, R. C., and Donahue, N. M.: Rapid growth of new atmospheric
485 particles by nitric acid and ammonia condensation, *Nature*, 581, 184-189,
486 <https://doi.org/10.1038/s41586-020-2270-4>, 2020.

487 Wennberg, P. O., Bates, K. H., Crounse, J. D., Dodson, L. G., McVay, R. C., Mertens, L. A., Nguyen, T.
488 B., Praske, E., Schwantes, R. H., Smarte, M. D., St Clair, J. M., Teng, A. P., Zhang, X., and Seinfeld, J.
489 H.: Gas-phase reactions of isoprene and its major oxidation products, *Chem. Rev.*, 118, 3337-3390,
490 <https://doi.org/10.1021/acs.chemrev.7b00439>, 2018.

491 Wu, K., Zhu, S., Liu, Y., Wang, H., Yang, X., Liu, L., Dabdub, D., and Cappa, C. D.: Modeling
492 ammonia and its uptake by secondary organic aerosol over China, *J. Geophys. Res. Atmos.*, 126,
493 e2020JD034109, <https://doi.org/10.1029/2020jd034109>, 2021.

494 Xie, H., Feng, L., Hu, Q., Zhu, Y., Gao, H., Gao, Y., and Yao, X.: Concentration and size distribution of
495 water-extracted dimethylaminium and trimethylaminium in atmospheric particles during nine
496 campaigns - Implications for sources, phase states and formation pathways, *Sci. Total Environ.*,
497 631-632, 130-141, <https://doi.org/10.1016/j.scitotenv.2018.02.303>, 2018.

498 Xu, L., Liu, X., Gao, H., Yao, X., Zhang, D., Bi, L., Liu, L., Zhang, J., Zhang, Y., Wang, Y., Yuan, Q.,
499 and Li, W.: Long-range transport of anthropogenic air pollutants into the marine air: Insight into fine
500 particle transport and chloride depletion on sea salts, *Atmos. Chem. Phys.*, 21, 17715-17726,
501 <https://doi.org/10.5194/acp-21-17715-2021>, 2021.

502 Yang, Z., Li, K., and Du, L.: Highly oxidized molecules make a significant contribution to enhanced
503 aromatic-derived secondary organic aerosol under a humid environment, *Adv. Atmos. Sci.*, 42, 641-652,
504 <https://doi.org/10.1007/s00376-024-4085-y>, 2025.

505 Yu, Z. and Li, Y.: Marine volatile organic compounds and their impacts on marine aerosol—A review,
506 *Sci. Total Environ.*, 768, 145054, <https://doi.org/10.1016/j.scitotenv.2021.145054>, 2021.



507 Zhang, R. and Chan, C. K.: Simultaneous formation of sulfate and nitrate via co-uptake of SO₂ and
508 NO₂ by aqueous NaCl droplets: Combined effect of nitrate photolysis and chlorine chemistry, Atmos.
509 Chem. Phys., 23, 6113-6126, <https://doi.org/10.5194/acp-23-6113-2023>, 2023.

510 Zhang, W., Ji, Y., Li, G., Shi, Q., and An, T.: The heterogeneous reaction of dimethylamine/ammonia
511 with sulfuric acid to promote the growth of atmospheric nanoparticles, Environ. Sci.: Nano, 6,
512 2767-2776, <https://doi.org/10.1039/c9en00619b>, 2019.

513 Zhang, W., Weber, J., Archibald, A. T., Abraham, N. L., Booge, D., Yang, M., and Gu, D.: Global
514 atmospheric composition effects from marine Isoprene emissions, Environ. Sci. Technol., 59,
515 2554-2564, <https://doi.org/10.1021/acs.est.4c10657>, 2025.

516 Zhou, S., Salter, M., Bertram, T., Brito Azevedo, E., Reis, F., and Wang, J.: Shoreline wave breaking
517 strongly enhances the coastal sea spray aerosol population: Climate and air quality implications, Sci.
518 Adv., 11, eadw0343, <https://doi.org/10.1126/sciadv.adw0343>, 2025.

519 Zou, Z., Chen, Q., Xia, M., Yuan, Q., Chen, Y., Wang, Y., Xiong, E., Wang, Z., and Wang, T.: OH
520 measurements in the coastal atmosphere of South China: Possible missing OH sinks in aged air masses,
521 Atmos. Chem. Phys., 23, 7057-7074, <https://doi.org/10.5194/acp-23-7057-2023>, 2023.

522